Available online at www.sciencedirect.com
ScienceDirect
Acta Biomaterialia 5 (2009) 2680–2692
Acta BIOMATERIALIA
www.elsevier.com/locate/actabiomat

The nanocomposite scaffold of poly(lactide-co-glycolide) and hydroxyapatite surface-grafted with L-lactic acid oligomer for bone repair

Yang Cui [a,b,c], Yi Liu [c], Yi Cui [a], Xiabin Jing [a], Peibiao Zhang [a,*], Xuesi Chen [a]

[a] State Key Laboratory of Polymer Physics and Chemistry, Changchun Institute of Applied Chemistry, Graduate School of Chinese Academy of Sciences, Chinese Academy of Sciences, Changchun 130022, People's Republic of China
[b] Changchun Central Hospital, Changchun 130051, People's Republic of China
[c] Department of Spine Surgery, First Hospital, Jilin University, Changchun 130021, People's Republic of China

Received 15 July 2008; received in revised form 11 February 2009; accepted 20 March 2009
Available online 27 March 2009

Abstract

Nanohydroxyapatite (op-HA) surface-modified with L-lactic acid oligomer (LAc oligomer) was prepared by LAc oligomer grafted onto the hydroxyapatite (HA) surface. The nanocomposite of op-HA/PLGA with different op-HA contents of 5, 10, 20 and 40 wt.% in the composite was fabricated into three-dimensional scaffolds by the melt-molding and particulate leaching methods. PLGA and the nanocomposite of HA/PLGA with 10 wt.% of ungrafted hydroxyapatite were used as the controls. The scaffolds were highly porous with evenly distributed and interconnected pore structures, and the porosity was around 90%. Besides the macropores of 100–300 μm created by the leaching of NaCl particles, the micropores (1–50 μm) in the pore walls increased with increasing content of op-HA in the composites of op-HA/PLGA. The op-HA particles could disperse more uniformly than those of pure HA in PLGA matrix. The 20 wt.% op-HA/PLGA sample exhibited the maximum mechanical strength, including bending strength (4.14 MPa) and compressive strength (2.31 MPa). The cell viability and the areas of the attached osteoblasts on the films of 10 wt.% op-HA/PLGA and 20 wt.% op-HA/PLGA were evidently higher than those on the other composites. For the animal test, there was rapid healing in the defects treated with 10 and 20 wt.% op-HA/PLGA, where bridging by a large bony callus was observed at 24 weeks post-surgery. There was non-union of radius defects implanted with PLGA and in the untreated group. This was verified by the Masson's trichrome staining photomicrographs of histological analysis. All the data extrapolated that the composite with 10 and 20 wt.% op-HA exhibited better comprehensive properties and were the optimal composites for bone repairing.

Keywords: Poly(lactide-co-glycotide); Grafted hydroxyapatite nanoparticles; Mechanical properties; Biocompatibility; Bone repair

1. Introduction

The development of resorbable composites has been the critical subject in developing bone substitute materials in surgical reconstruction and bone tissue engineering in recent years. The composites of hydroxyapatite nanoparticles and poly(lactide) (HA/PLA) or poly(lactide-co-glycotide) (HA/PLGA) have attracted considerable attention due to their good osteoconductivity and biodegradability, and their high mechanical strength [1–3]. In particular, more and more research has been focused on the PLGA materials because their degradation rate can be adjusted by altering the ratio of lactic to glycolic acids. This is a desirable characteristic due to the fact that the rate of bone formation is dependent upon both the size and the site of the defect [2]. However, the lack of adhesion between the HA nanoparticles and PLGA matrix resulted in early failure at the HA–polymer interface, thus deteriorating the

* Corresponding author. Tel.: +86 431 85262390; fax: +86 431 85685653.
E-mail address: zhangpb@ciac.jl.cn (P. Zhang).

1742-7061/$ - see front matter © 2009 Acta Materialia Inc. Published by Elsevier Ltd. All rights reserved.
doi:10.1016/j.actbio.2009.03.024

mechanical properties [4]. It is therefore necessary to develop materials with higher mechanical strength to satisfy clinical requirement of repairing load-bearing bone defects.

To improve this situation, various methods have been developed to improve adhesion between HA and polymeric matrix, such as surface modification of HA particles with silane coupling agents [5], zirconyl salt [6], poly acids [7], dodecyl alcohol [8], polyethylene glycol [9] and isocyanate [10]. In these techniques, the coupling agent molecules were chemically reacted with the hydroxyl groups on the surface of the HA and thus the affinity of the particle surface to the PLA matrix was improved significantly. However, most of the grafted organic molecules as mentioned above are usually noxious.

The previous works of our group were focused on in situ grafting ring-opening polymerization of L-lactide (LLA) onto the surface of HA particles [4,11–13]. Stannous octanoate (Sn(Oct)2) was selected as a catalyst in these reactions for its low toxicity and high reactivity. Improved interface compatibility, mechanical properties and biocompatibility of the nanocomposites of HA/PLA or HA/PLGA with grafted HA particles were obtained.

A new method of modifying the surface of hydroxyapatite nanoparticles has been developed that involves the surface grafting reaction of L-lactic acid oligomer (LAc oligomer) (op-HA) in the absence of any catalyst and coupling agent [14]. The property of interface adhesion between the op-HA and the polymer matrix and the mechanical properties of the composite were improved significantly.

To investigate its further applications in orthopedics and tissue engineering, the nanocomposite of op-HA/PLGA with various op-HA ratios was fabricated into three-dimensional (3D) scaffolds by a melt-molding particulate-leaching method. The mechanical strength, biocompatibility and osteogenetic activity of the composites were studied in vitro and in vivo. The comparison of the composites with various contents of op-HA in physicochemical properties and biological properties was undertaken.

2. Materials and methods

2.1. Preparation of op-HA/PLGA composites

Poly(lactide-co-glycolide) (PLGA, LA:GA = 8:2, Mw = 100,000) was synthesized in our laboratory. The preparations of hydroxyapatite (HA) and LAc oligomer surface grafted HA (op-HA) nanocrystals have been reported in our previous work [14]. Briefly, HA nanocrystals 100–200 nm in length and 20–30 nm in width were hydrothermally synthesized according to the reaction equation (Eq. (1)):

$$6H_3PO_4 + 10Ca(OH)_2 \rightarrow Ca_{10}(PO_4)_6(OH)_2 + 18H_2O \quad (1)$$

The Lac oligomer with a certain molecular weight was directly synthesized by condensation of L-lactic acid, and grafted onto the HA surface by forming a Ca carboxylate bond in the absence of any catalyst according to the reaction equation (Eq. (2)).

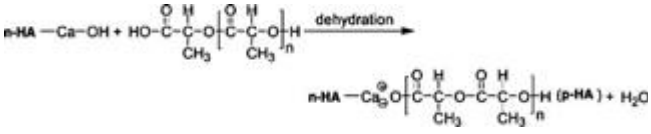

(2)

The amount of grafted LAc oligomer in op-HA used in this study is about 10 wt.% analyzed with the method of weight loss using the thermogravimetry analysis (TGA) (TA Instruments TGA500, USA).

The op-HA/PLGA composites with various amounts of op-HA (5, 10, 20 and 40 wt.%) and the HA/PLGA composite with 10 wt.% of HA were prepared by the solvent-mixing method. Briefly, the dried op-HA powders were uniformly suspended in 20-fold (by wt.) chloroform with magnetic stirring and ultrasonic treatment. The suspension was added into a 5% PLGA/chloroform solution to achieve the op-HA content of 5–40 wt.% in the composites. The mixture was precipitated in an excess of ethanol, and the composite was dried in air for 48 h and vacuumed for 72 h to remove the residual solvent. HA/PLGA composite was prepared according to the above-mentioned method.

2.2. Fabrication of porous op-HA/PLGA

The porous scaffolds were fabricated by a melt-molding particulate leaching method according to Ref. [15]. Briefly, sieved sodium chloride particulates 100–300 μm in diameter were added into melted PLGA and op-HA/PLGA (5, 10, 20 and 40 wt.%) or HA/PLGA in an internal mixer at 150 °C and 60 rpm. The weight ratios of salt particulates to the composites were 6:1. The blends were then molded into 3-mm-thick sheets, respectively, under 10 MPa pressure at 150 °C for 5 min, and cooled to room temperature. The salt particles were subsequently removed from the molds by leaching in distilled water for 10 days, and the water was changed every 12 h. Then the porous composites were air-dried for 48 h and vacuumed for 24 h. The porous scaffolds were obtained, and sterilized with ethylene oxide for 4 h.

2.3. Environmental scanning electron microscopy (ESEM) observation

An environmental scanning electron microscope (Model XL 30 ESEM FEG, Philips) was used to observe the morphology in the fracture surface of the porous scaffolds of PLGA, op-HA/PLGA (5, 10, 20 and 40 wt.%) and HA/PLGA. The scaffolds were frozen in liquidized N_2, and quickly broken off to obtain the random brittle-fractured

surface. A layer of gold was sprayed uniformly over the fractured surfaces before the observation.

2.4. Determination of the porosity

The porosity of the scaffolds was measured by the method of modified liquid displacement with absolute ethanol according to the literature [16]. Briefly, a scaffold sample was immersed in a graduated test tube containing a known volume (V_1) of ethanol. The sample was kept in ethanol for 5 min and then vacuumed to evacuate the air, allowing the ethanol into pores of the porous scaffold. This process was continued until no air bubbles emerged from the scaffold. The total volume of the ethanol and scaffold was then recorded as V_2. The ethanol-impregnated scaffold was removed carefully from the test tube and the residual ethanol volume in the test tube recorded as V_3. The volume of the ethanol held in the foam was $(V_1 - V_3)$, which was determined as the void volume of the scaffold. The total volume of the scaffold was $(V_2 - V_3)$. The porosity of the scaffold (ε) was calculated by: $\varepsilon = (V_1 - V_3)/(V_2 - V_3)$. The average of three measurements was taken for each sample.

2.5. Bending strength and compressive strength tests

Rectangular bars of 30 mm×5 mm×3 mm were used for mechanical strength tests measured by a universal testing machine (Instron 1121, UK). The three-point bending strength was measured at a crosshead speed of 5 mm min^{-1}. Meanwhile, the compressive strength was measured at a crosshead speed of 2 mm min^{-1}. The stress histogram was obtained to determine mechanical properties. Three replicates were tested for each condition ($n = 3$).

2.6. Cell culture

A full-thickness skull was obtained from a newborn rabbit and rinsed three times with 0.1 M PBS, and the fibrous tissues were removed. The skull was then chipped into small pieces (1.0 mm×1.0 mm in size) and placed at the bottom of a cell culture dish (100 mm×20 mm style), then cultured with Dulbecco's modified Eagle's medium (DMEM, Gibco) supplemented with 20% FBS (Gibco), 10 mM Hepes (Sigma), 60 mg l^{-1} penicillin (Sigma) and 100 mg l^{-1} streptomycin (Sigma) in a humidified incubator at 37 °C and 5% CO_2. The medium was changed every 2 days. After 1 week of culture, the monolayer osteoblasts developed and expanded from the skull pieces. The osteoblasts were removed from the cell culture dishes by trypsin (2.5 mg ml^{-1}) and EDTA (0.2 mg ml^{-1}) (1:1, v/v) treatment, then rinsed three times with 0.1 M PBS by centrifugation at 1000 rpm for 5 min.

2.7. Cell attachment and spreading

Cell attachment and spreading of osteoblasts on PLGA, op-HA/PLGA (5, 10, 20 and 40 wt.%) and HA/PLGA were analyzed by NIH Image J software. Samples of the scaffolds (100 mg) were dissolved in 10 ml chloroform to form a 1 wt.% homogeneous solution. The solution (30 μl) was then coated onto 24 mm×24 mm cover slides that had been pretreated with 2% dimethyl dichlorosilane (DMDC, Fluka) and heated at 180 °C for 4 h before use. The cover slides were vacuum-dried for 48 h at room temperature and then sterilized with UV radiation for 30 min. The obtained osteoblasts were resuspended in the medium, seeded on the cover slides in 6-well cell culture plates (Costar) at a density of 2.5×10^4 cells ml^{-1} and cultured at 37 °C in 5% CO_2 for 1, 3, 5 and 7 days, respectively. The cover slides were taken out at different time intervals and washed three times with PBS. The cells were dyed with 0.5 mg ml^{-1} fluorescent isothiocyante (FITC, Sigma) for 5 min and washed with PBS three times. The morphology of the cells attached and spread on each sample was observed with an inverted fluorescence microscope (TE 2000U, NIKON). Nine pictures of each cover slide were taken by a digital camera (DXM 1200F, NIKON) and analyzed by NIH Image J. The average area fraction of osteoblasts on each biomaterial was obtained.

2.8. Cell viability

The cell viability of the osteoblasts on the above-mentioned materials was assayed using the 3-(4,5-dimethylthiazoyl-2-yl)-2,5-diphenyltetrazolium bromide (MTT) method [17], which was used in our study to quantitatively assess the number of viable cells attached and grown on the material surface.

Six groups of materials (virgin PLGA, 5, 10, 20 and 40 wt.% op-HA/PLGA and HA/PLGA) were molded into films of 0.1 mm thickness by the solvent casting method [18]. The films were cut into disks 4.5 mm in diameter and sterilized under UV radiation for 30 min. Disks of six samples were placed in the wells of 96-well tissue culture plates (Costar). The bottom surface of the wells was fully covered by the disk. Six replicates were used for each sample. Briefly, the osteoblasts (0.5×10^4 cells in 200 μl medium) were incubated in 96-well plates at 37 °C and 5% CO_2 for 1, 3, 5 and 7 days, respectively. The medium was changed every 2 days. Four hours before each culture interval, 20 μl of MTT (5 mg ml^{-1} in PBS) was added to each well and the cells were incubated for an additional 4 h. The medium was removed and 200 μl of acidified isopropanol (0.2 ml of 0.04 N HCl in 10 ml of isopropanol) was added to each well to solubilize the converted dye. The solution (150 μl) in each well was mixed and transferred to another 96-well plate, and optical density was measured at 540 nm wavelength on a Thermo Electron MK3 spectrophotometer. The mean value of the six readings for each sample was used as the final result.

2.9. Repair for rabbit radius defects

The PLGA, HA/PLGA and op-HA/PLGA (5, 10, 20 and 40 wt.%) porous scaffolds were implanted into rabbit

radius defects. Twenty-two rabbits, weighing an average of 2.5 kg, were selected for the animal test. An approximately 3-cm-long incision was made, and the tissues overlying the distal diaphyseal radius were dissected. A 2.0 cm segmental defect was cut in the bilateral radius by a mini-oscillating saw. In the untreated group, nothing was implanted in the defect for the control. Three replicates were set for each group.

Animals were kept in the Institute of Experimental Animal of Jilin University, in accordance with the institutional guidelines for care and use of laboratory animals. Anterioposterior radiographs of each limb were taken on KODAK CR 400 plus Filmeless Radiology system (USA) at 4 and 24 weeks after operation to follow the healing process at the resection sites.

2.10. Histological analysis

The rabbits were sacrificed by an overdose of anesthesia at 24 weeks post-surgery. The implanted forearms and surrounding tissues were harvested and fixed with 4% paraformaldehyde for 24 h. The samples were decalcified in 10% EDTA for 4 weeks, embedded in paraffin and cut into 5-μm-thick slices using a Microtome. The slices were stained with Masson's trichrome staining and evaluated under light microscopy.

2.11. Statistical analysis

The data were expressed as means ± standard deviation. Statistical analysis was performed with SPSS11.5 software. One-way analysis of variance was used to compare two different groups. A p value of <0.05 was considered to be statistically significant.

3. Results and discussion

3.1. Scaffold characterization

The structures of the porous scaffolds of PLGA, op-HA/PLGA and HA/PLGA fabricated with the melt-molding particulate leaching method were observed by ESEM. The micrographs of the scaffolds are shown in Figs. 1–3. All scaffolds were highly porous with evenly distributed and interconnected pore structures (Fig. 1). Two levels of pores were observed in all scaffolds: interconnected macropores 100–300 μm in diameter, created by the leaching of NaCl particles; and closed micropores 1–50 μm in diameter, which appeared in the walls of macropores (Figs. 1 and 2). There were more micropores in the nanocomposite scaffolds of HA/PLGA (Fig. 2F) and op-HA/PLGA (Fig. 2B–E) compared to PLGA (Fig. 2A). Moreover, the micropores increased with the content of op-HA in the composites of op-HA/PLGA (Fig. 2B–E). According to the literature, similar micropores were found in the composite scaffolds of HA/PLGA fabricated by the gas forming and particulate leaching (GF/PL) method, and the bone regeneration was enhanced with this kind of scaffolds [3]. Thus, it is deduced that the micropores may impact on not only mechanical properties but also osteogenesis of scaffolds, and possible reasons for the micropore formation are the resident solvent and the viscosity increasing of nanocomposites.

Compared to the solvent casting and particulate leaching method reported in our previous work [19] and the literature [20], the melt-molding and particulate leaching method in this study produced more strict architecture of the scaffolds due to melt-molding with high pressure and processing in the absence of solvent (Fig. 1). The surface modification of HA seemed to improve the architecture of the composites because op-HA/PLGA (Fig. 1B–E) exhibited better pore structure than ungrafted HA/PLGA (Fig. 1F).

The porosity values of the scaffolds measured by the method of liquid displacement are listed in Table 1. The porosities of both PLGA and HA/PLGA were around 87%. Although the content of op-HA in op-HA/PLGA influenced the porosities of the scaffolds to some extent, there were no significant differences compared to PLGA and HA/PLGA ($p > 0.05$). As the op-HA content was 5 wt.%, the porosities of the composite scaffolds of op-HA/PLGA decreased slightly compared to the pristine PLGA. As the op-HA content was increased to 10 and 20 wt.%, the porosities of the composite scaffolds increased to around 91–93%, and were higher than those of the pristine PLGA and ungrafted HA/PLGA. Conversely, as the op-HA content reached 40 wt.%, the porosities decreased. According to the micrographs of SEM, the porosity decreasing of 40 wt.% op-HA/PLGA may result from thicker pore walls and the increasing of closed micropores in the walls.

It was reported that the surface topography is important for cell attachment. Surface roughness of the pore wall enhances attachment, proliferation and differentiation of anchorage-dependent bone forming cells [21]. In this study, it was observed that the composite scaffolds of op-HA/PLGA (Fig. 3B–E) and HA/PLGA (Fig. 3F) exhibited rougher pore walls due to the particles attached or inlaid on the surface of the wall compared to PLGA (Fig. 3A). The roughness of the pore walls increased as the content of op-HA in op-HA/PLGA increased from 5 to 40 wt.% (Fig. 3B–E). Moreover, the grafted op-HA particles dispersed more uniformly on the surface of pore walls in 10 and 20 wt.% op-HA/PLGA (Fig. 3C and D) than ungrafted HA in PLGA matrix (Fig. 3F). More agglomerated particles (as indicated by the arrows in Fig. 3F) were found in ungrafted HA/PLGA composites. Meanwhile, there were flatter surfaces on the pore walls of the 10 and 20 wt.% op-HA/PLGA than on the walls of the others. This indicates that the surface modification of HA grafted with LAc oligomer could improve the distribution of the nanoparticles in the PLGA matrix more uniformly than the ungrafted HA. The compositions of the 10 and 20 wt.% op-HA/PLGA provide more uniform roughness and a flat surface for cell attachment and immigration.

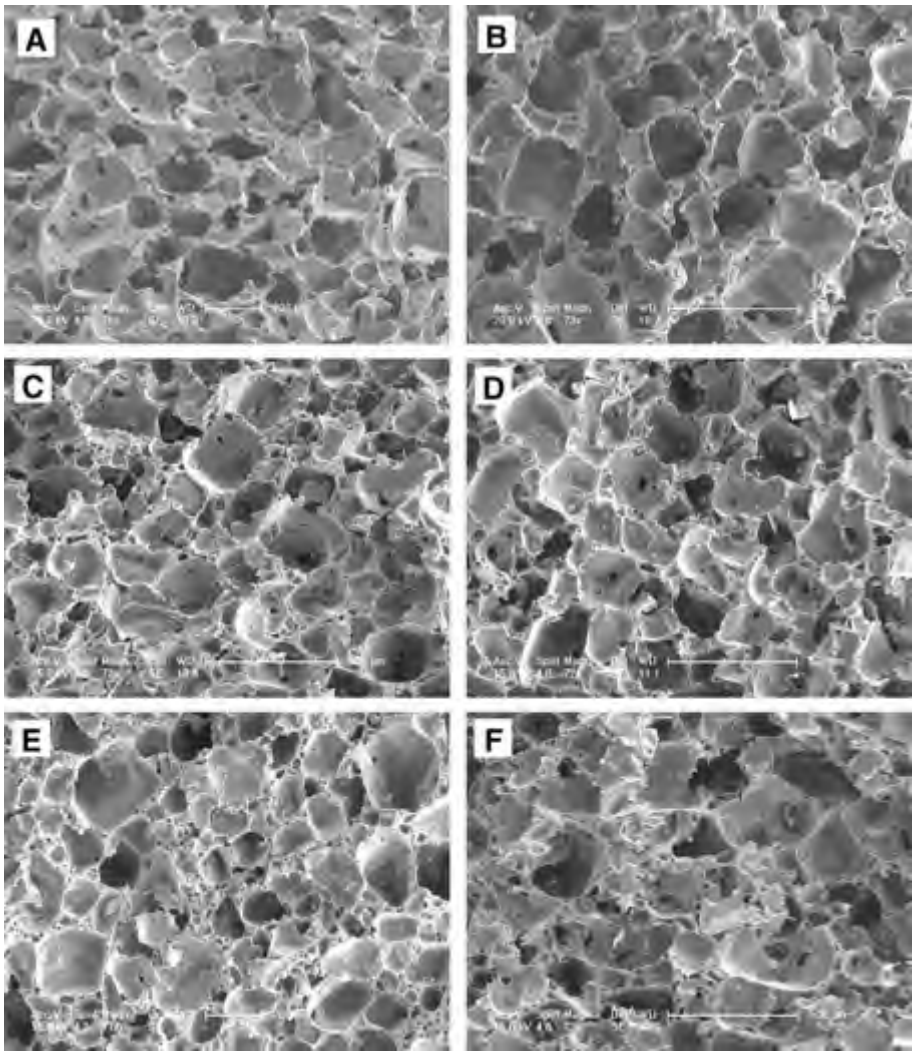

Fig. 1. SEM micro-photographs of porous scaffolds of: PLGA (A), 5 wt.% op-HA/PLGA (B), 10 wt.% op-HA/PLGA (C), 20 wt.% op-HA/PLGA (D), 40 wt.% op-HA/PLGA (E) and HA/PLGA (F) fabricated with the melt-molding particulate leaching method. Scale bar lengths are 200 μm (A and E), 500 μm (B, C, D and F).

3.2. Mechanical properties

Mechanical properties of the porous scaffolds of PLGA, op-HA/PLGA and HA/PLGA were evaluated by bending and compressive strength measurement (Fig. 4). The relationship between the bending strength and the content of op-HA filler in composites is demonstrated in Fig. 4A. At the lower filler content (5 wt.%), there was a slight decrease in the bending strength compared with PLGA. The values increased with increasing amounts of op-HA filling particles (10 and 20 wt.%). The 20 wt.% op-HA/PLGA sample exhibited a maximum strength (about 4.14 MPa) and was statistically different from the other groups ($p < 0.05$). However, the bending strength decreased obviously when the filler content was 40 wt.%. The 10 and 20 wt.% op-HA/PLGA composites showed higher bending strength than HA/PLGA and PLGA, but there was no statistical difference between 10 wt.% op-HA/PLGA and HA/PLGA or PLGA.

The relationship between the inorganic particle content and the compressive strength for the op-HA/PLGA composites is illustrated in Fig. 4B. The dependency trend of the composites was similar with the bending strength. At the lower filler content (5 wt.%), there was a slight decrease in the compressive strength compared with PLGA. The values increased with increasing amounts of op-HA filling particles (10 and 20 wt.%). The 20 wt.% op-HA/PLGA sample reached a maximal value (about 2.3 MPa) and was statistically different from the other groups ($p < 0.05$). However, the compressive strength decreased obviously when the filler content was 40 wt.%. The 10 wt.% op-HA/PLGA composite showed higher compressive strength than HA/PLGA, but there was no statistical difference between the two composites.

These data indicate that grafting modification of HA did show significant influence on improving mechanical properties of the composite at a certain content, because the op-HA particles could be dispersed more easily and homogeneously in the composite than corresponding HA. The grafted LAc

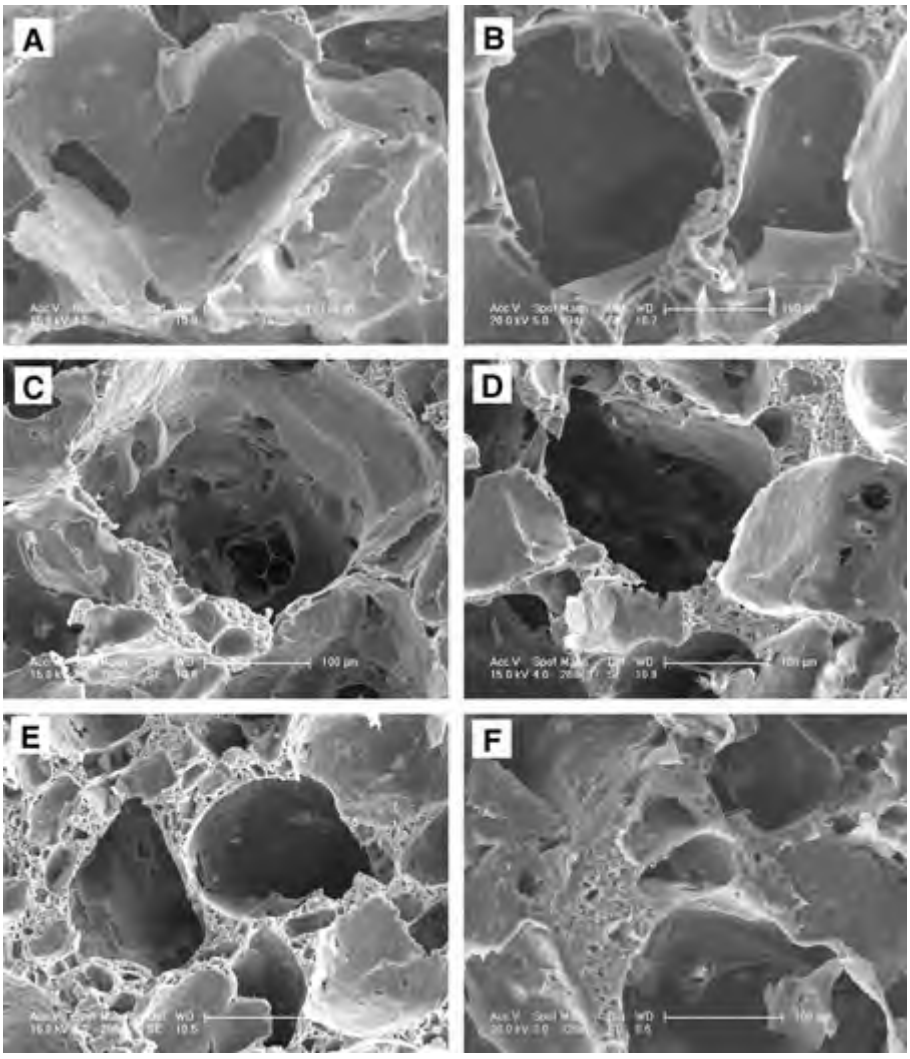

Fig. 2. SEM micro-photographs of porous scaffolds of: PLGA (A), 5 wt.% op-HA/PLGA (B), 10 wt.% op-HA/PLGA (C), 20 wt.% op-HA/PLGA (D), 40 wt.% op-HA/PLGA (E) and HA/PLGA (F) fabricated with the melt-molding particulate leaching method. Scale bar lengths are 100 μm.

oligomer molecules can enter into the PLGA matrix as anchors to mix tightly, crystallize and entangle with the molecular chains of PLGA matrix, thus the op-HA particles are strongly tethered to matrix in the op-HA/PLGA composites [14]. The proportion of inorganic filler in the composite is of importance to the mechanical properties of the composite [2,4,12–14,20]. The similar appearances are shown in natural bone. In this study, the optimal proportion of op-HA particles in the composite is 20 wt.%, which exhibited the highest bending and compressive strength. Increasing the inorganic composition extremely would make the composites brittle and decrease the strength remarkably. According to the SEM observation, the forming of micropores in the pore walls may be another important factor to impact on the mechanical properties of the composite.

3.3. Cellular responses

The attachment and spreading of osteoblasts on materials are shown in Figs. 5 and 6. Fig. 5 shows the representative fluorescent photographs of osteoblasts cultured on PLGA, 20 wt.% op-HA/PLGA and 10 wt.% HA/PLGA and in vitro for 1, 3, 5 and 7 days, respectively. The cells initially attached and spread better on the composite of op-HA/PLGA and HA/PLGA than PLGA after 1–3 days' culture. After culturing for 5–7 days, the attached cells proliferated and spread actively, covering most of the surface. There were more cells grown on op-HA/PLGA than on PLGA and HA/PLGA. The cells on 20 wt.% op-HA/PLGA seemed to grow better than other op-HA/PLGA composites. However, the cell morphology of the osteoblasts on 20 wt.% op-HA/PLGA was similar to that of the osteoblasts on PLGA, HA/PLGA and the other op-HA/PLGA composites (data not shown).

Fig. 6 displays the area fraction of osteoblasts spreading on different materials analyzed by NIH Image J software. The cell area fraction in pure PLGA was lower than that in the composites with op-HA or HA at all time intervals. At 1 day culture, there were only a few cells attached on the materials for a lower area fraction (<2.5%). The cell

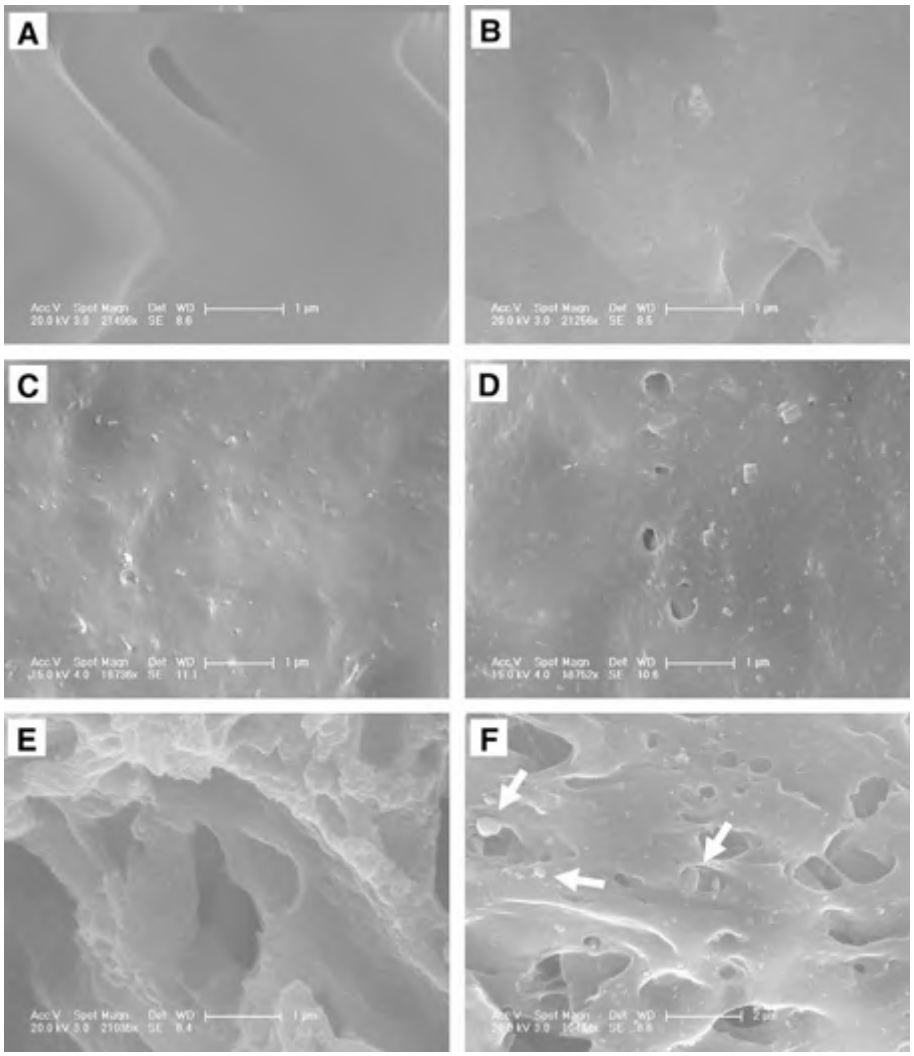

Fig. 3. The surface tomography of the pore walls of the porous scaffolds of: PLGA (A), 5 wt.% op-HA/PLGA (B), 10 wt.% op-HA/PLGA (C), 20 wt.% op-HA/PLGA (D), 40 wt.% op-HA/PLGA (E) and 10 wt.% HA/PLGA (F). Scale bar lengths are 1 μm (A–E) and 2 μm (F).

Table 1
The porosity of porous scaffolds fabricated with the melt-molding/particulate leaching method.

Composites	Porosity (mean ± SD, %)
PLGA	87 ± 6
5% op-HA/PLGA	84 ± 4
10% op-HA/PLGA	91 ± 5
20% op-HA/PLGA	93 ± 4
40% op-HA/PLGA	86 ± 8
HA/PLGA	88 ± 7

amount on PLGA was less than that of HA/PLGA, but there was maximum quantity on 20 wt.% op-HA/PLGA. At 3 and 5 days' culture, the cells began to proliferate and spread on the materials. The spreading area of cells on 20 wt.% op-HA/PLGA was markedly larger than that on the other composites, and the cells' area of PLGA is less than that of HA/PLGA. At 7 days' culture, the cells proliferated and spread favorably on the composites. The cells covered the most areas of the cover slide on 20 wt.% op-HA/PLGA. The spreading area of cells on 20 wt.% op-HA/PLGA was markedly larger than that on the other materials, and the difference was statistically significant ($p < 0.05$). The obtained results of the area fraction are in good agreement with the optical observation of the above-mentioned fluorescent photographs.

The cell viability of osteoblasts on the different materials using MTT assay is shown in Fig. 7. On 10 wt.% op-HA/PLGA, the proliferation level of cells was evidently higher than that on the other materials; the difference was significant ($p < 0.05$). After culturing for 7 days, there was no significant difference about the proliferation and spreading areas of cells between 10 wt.% op-HA/PLGA and 20 wt.% op-HA/PLGA. The cell attachment and proliferation of 10 wt.% op-HA/PLGA were better than corresponding HA/PLGA.

On all accounts, as for 10 wt.% op-HA/PLGA and 20 wt.% op-HA/PLGA, the proliferation level and the areas of the spreading osteoblasts were evident higher than on the other composites.

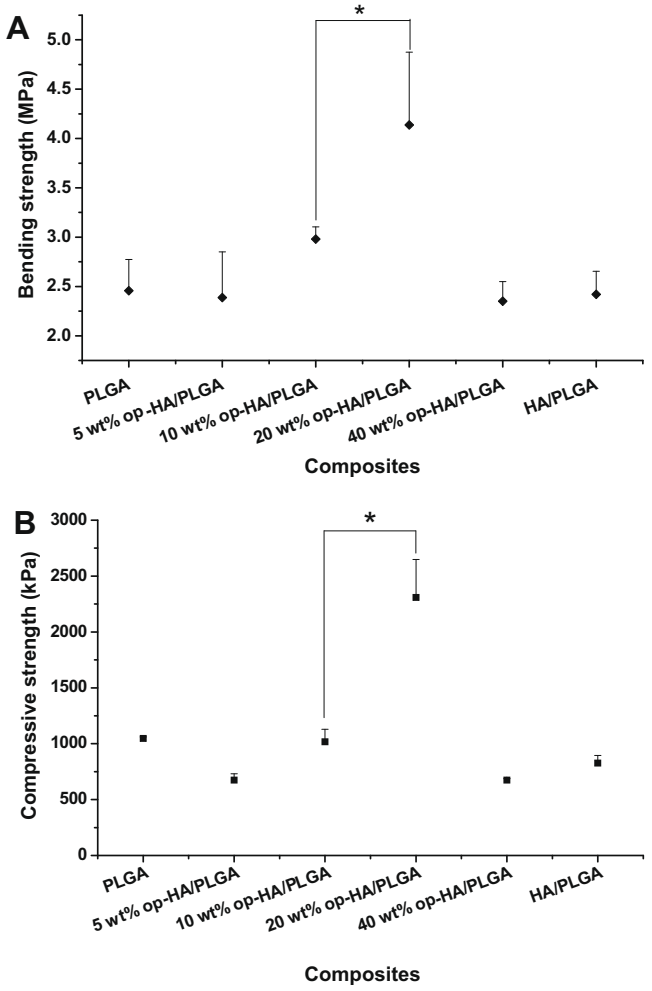

Fig. 4. Dependence of bending strength (A) and compressive strength (B) on the filler of op-HA or HA content in the composite scaffolds.

It has been well known that cell adhesion is an important cellular behavior because it directly affects proliferation. Both osteoblast adhesion and proliferation on the composite are very important factors for osteogensis. As a result, the cell behavior and interaction with a bioactive material surface are dependent on properties such as topography, surface charge and chemistry [22,23]. The composite of HA/PLA or PLGA has shown good biological properties as potential material for orthopedic application. The samples of 20 wt.% op-HA/PLGA covered the greatest area fraction and 10 wt.% op-HA/PLGA obtained maximal proliferation after 7 days' culture. However, the composite (40 wt.% op-HA/PLGA) containing high content op-HA particles did not show higher cell attachment and proliferation abilities. The results implied that an ideal composite should promote the cell growth, and the explanation may be contained in the following three aspects.

First, the op-HA or HA particles in PLGA may have positive biological effects because op-HA particles formed a rough surface. The rough surface could have a positive impact on the adherence of the cells [24,25]. In addition, the op-HA particles disengaged from composite and exposed to body fluid might induce a microenvironment change, i.e. the alkalinization of the medium, which has a positive influence on cell metabolism [26]. Second, the composite of HA/PLGA or op-HA/PLGA possesses a greater ability of cell adhesion and proliferation compared with pristine PLGA, and op-HA particles could disperse in the matrix more homogeneously than HA particles; thereby, the cell attachment and proliferation on op-HA/PLGA was better. Lastly, the acid products degraded from the op-HA/PLGA will impact on the cell behaviors on the materials. In this study, the nanoparticles of op-HA contained 10% (w/w) L-lactic acid oligomer, which was easy to detach from the nanoparticles by hydrolysis. Increasing op-HA content in the composite would produce more acid products (such as L-lactic acid oligomer and lactic acid) in a short period, which could induce inflammatory responses to influence the cellular adherence, proliferate and spread on the surface of materials. Thus the result that 40 wt.% op-HA/PLGA acquired a smaller cellular adhesion area than 20 wt.% op-HA/PLGA could be explained.

3.4. Implantation for repair bone defects

The critical size defect has been widely used in animal models for evaluating bone healing. It is the smallest diameter intraosseous wound that would not heal spontaneously. The suggested critical size defect in rabbit is 15 mm [27]. In this study, the length of rabbit radius defects was 20 mm, and the radiographic results proved that the defects of untreated control could not be bridged naturally.

During the observation period, all animals were healthy and presented no signs of infection. The healing of the radius defects was assessed radiologically and histologically after experimental times of 4 and 24 weeks.

3.4.1. Radiographic evaluation

Typical radiographs of the rabbit radius defects implanted with porous scaffolds of PLGA, HA/PLGA and op-HA/PLGA with different contents of op-HA at 4 and 24 weeks post-surgery are shown in Fig. 8.

At 4 weeks post-surgery, distinct bone callus emerged at the defect areas in the groups of HA/PLGA, and 10 and 20 wt.% op-HA/PLGA (Fig. 8E1, F1 and G1). However, there was only a small quantity of bone callus at the ends of defect areas near to the neighboring bone in the groups of the untreated control, PLGA, and 5 and 40 wt.% op-HA/PLGA (Fig. 8A1, B1, C1 and G1).

At 24 weeks post-surgery, the defects in the groups of HA/PLGA and 5–40 wt.% op-HA/PLGA were bridged by new bones (Fig. 8C2, D2, E2, F2 and G2), while the pure PLGA and untreated groups had only limited ability to induce bone callus formation at the ends of bone defects and failed to unite (Fig. 8A2 and B2). Only the defects treated with 10 and 20 wt.% op-HA/PLGA (Fig. 8D2 and E2) developed a larger calcified callus, and the planimetric volumes of callus in these two groups were nearly 2–3 times larger than those of others. By contrast, the defects treated

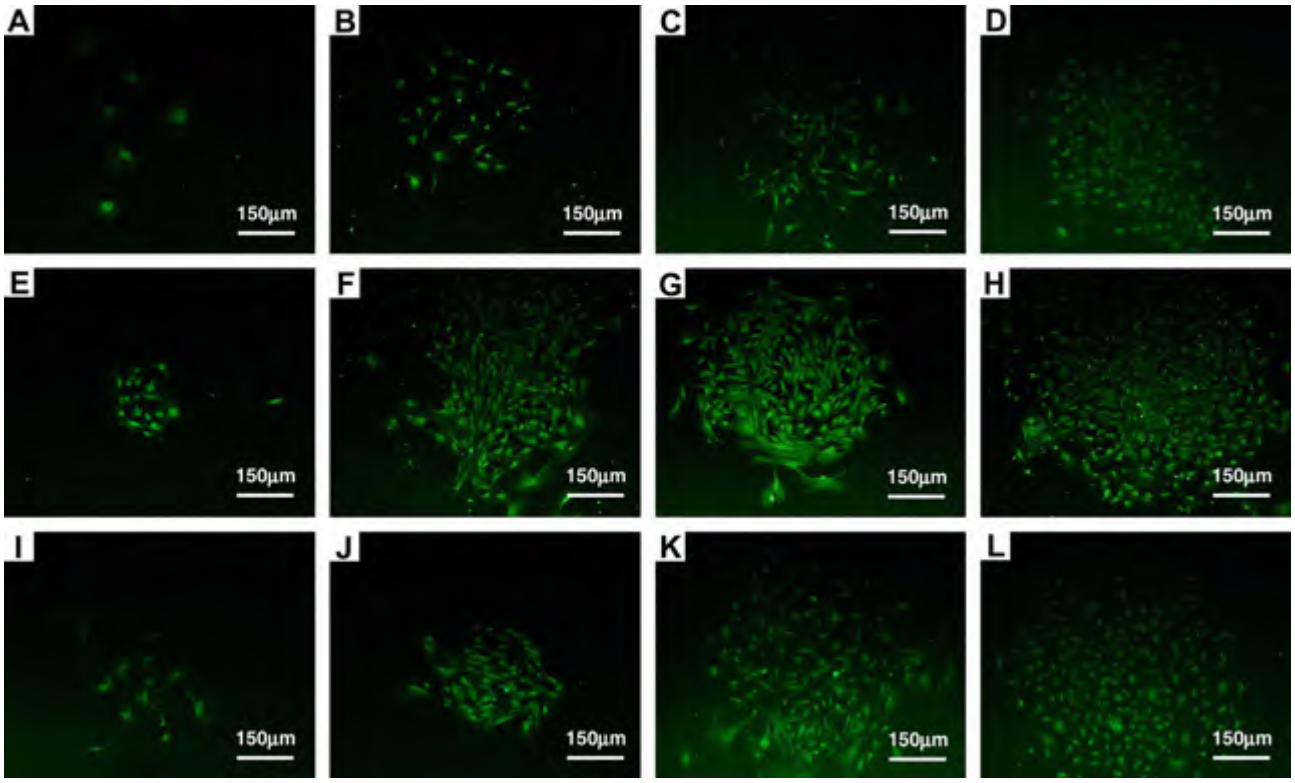

Fig. 5. Fluorescent photographs of osteoblasts adhered on the membranes of: PLGA (A–D), 20 wt.% op-HA/PLGA (E–H) and HA/PLGA (I–L) cultured for 1 (A, E and I), 3 (B, F and J), 5 (C, G and K) and 7 (D, H and L) days.

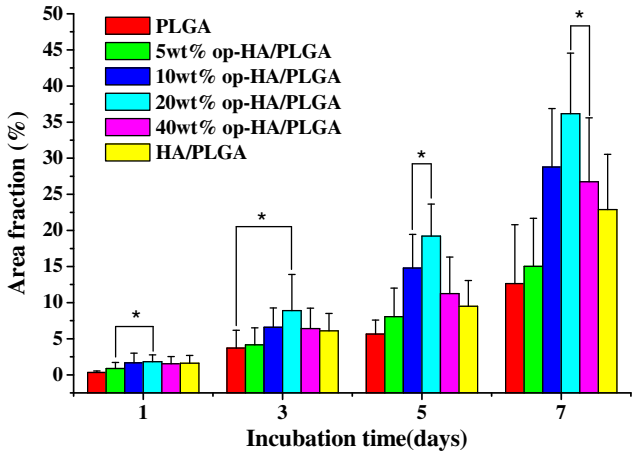

Fig. 6. Osteoblast adhesion analysis with NIH Image J software ($^{*}p < 0.05$).

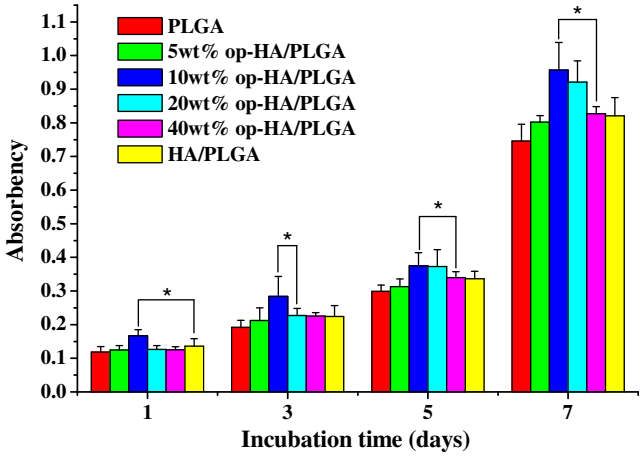

Fig. 7. Osteoblast proliferation analysis by MTT test ($^{*}p < 0.05$).

with 5 and 40 wt.% op-HA/PLGA, and HA/PLGA developed less bone callus along the composites (Fig. 8C2 and F2).

According to the radiographic results, PLGA showed limited osteoconductivity although it is of good biocompatibility. The osteoconductive ability was improved greatly by the incorporation of bioactive HA or op-HA into the PLGA matrix. Moreover, the osteoconductivity of op-HA/PLGA was obviously influenced by the content of op-HA, with the 10 and 20 wt.% op-HA/PLGA exhibiting the highest osteoconductivity and the best quality of bone healing. The results may be associated with a number of factors, such as the surface tomography, mechanical properties and microstructure of the porous scaffolds.

3.4.2. Histological analysis

Fig. 9 shows representative histological micrographs of the repaired areas with Masson's trichrome staining at 24 weeks after implantation. Prominent capillary proliferation was detected in all groups. The scaffolds were mostly degraded and replaced with several types of cells and a

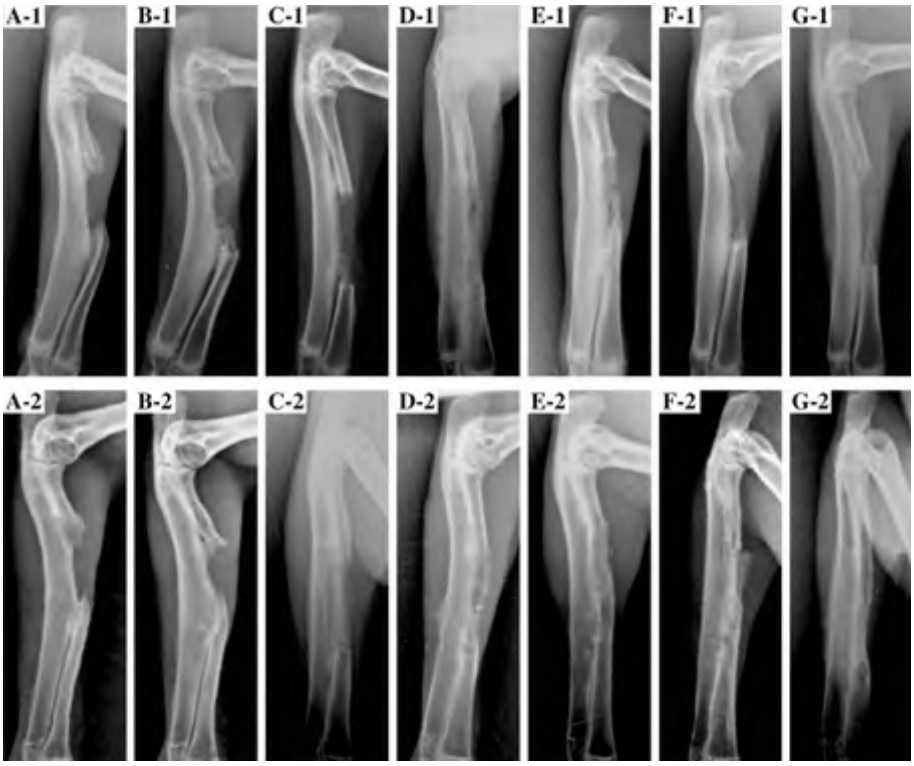

Fig. 8. Typical radiographs of radius resection implanted with composites: untreated control (A1&2), PLGA (B1&2), 5 wt.% op-HA/PLGA (C1&2), 10 wt.% op-HA/PLGA (D1&2), 20 wt.% op-HA/PLGA (E1&2), 40 wt.% op-HA/PLGA (F1&2) and HA/PLGA (G1&2) taken at 4 (1) and 24 (2) weeks post-surgery.

large quantity of extracellular matrices. In the 10 and 20 wt.% op-HA/PLGA groups, the defects were almost filled with bone ossein (Fig. 9C and D). Only a small quantity of bone ossein and capillaries were observed in the HA/PLGA (Fig. 9F), 5 and 40 wt.% op-HA/PLGA groups (Fig. 9B and E). However, in the PLGA group, the defect area was nearly filled with fibrous tissues (Fig. 9A).

There were more small oval-shaped mononuclear cells (osteoblasts) and multinucleated-giant cells observed in the composite implants of op-HA/PLGA (Fig. 9B–E) and HA/PLGA (Fig. 9F) than in PLGA (Fig. 9A). The multinucleated-giant cells in the 40 wt.% op-HA/PLGA group were found to be the most numerous and most active around the bone ossein. This indicates that osteoblasts could grow into the pores of materials and secrete bone ossein to form trabecular bone. At the same time, the multinucleated-giant cells and osteoclasts might swallow the composites to improve the degradation for cell ingrowth and new bone formation. In the 40 wt.% op-HA/PLGA group, a number of factors seem to delay or hinder new bone formation and degradation of the composites. The histological analysis provided further evidence to explain why the 10 and 20 wt.% op-HA/PLGA exhibited the highest osteoconductivity and the best quality of bone healing according to the radiographic results.

The interconnected highly porous structure of op-HA/PLGA, with interconnections averaging 100–300 μm in diameter, allows efficient migration of bone-producing cells from pore to pore, as well as the invasion by vascular vessels that is essential for new bone formation. Because of its high porosity and good strength, its 3D structure is preserved whole throughout the repair process, offering a good scaffold for bone ingrowth. The PLGA used in this study is biocompatible and biodegradable, with little inflammatory potential; thus, it does not interfere with new bone formation in the pores. Obviously, the lack of bony repair alone in the PLGA group demonstrates the importance of HA or op-HA in the repair process.

HA has already been shown to be both biocompatible and osteoconductive [28]. As a natural component of bone, hydroxyapatite synthesized on the nanometric scale seems structurally more similar to the apatite in bone, and it possesses the ability to promote the attachment and proliferation of osteoblasts, and subsequently improves their metabolic activity [29,30]. The bioactivity of HA is likely due to the binding of serum proteins [31] and growth factors [32], and the adhesion and proliferation of osteoblasts may be promoted. Thus, HA has great potential application in tissue engineering and clinical orthopedics.

The surface modification of HA with L-lactic acid oligomer provided a new method to improve the interface adhesion of the composites and the distribution of op-HA in polymer matrix [14]. The novel composites of grafted HA and PLA or PLGA were initially designed to be used as bone fixation materials due to their improved mechanical properties [12–14]. At first, we were worried that the sur-

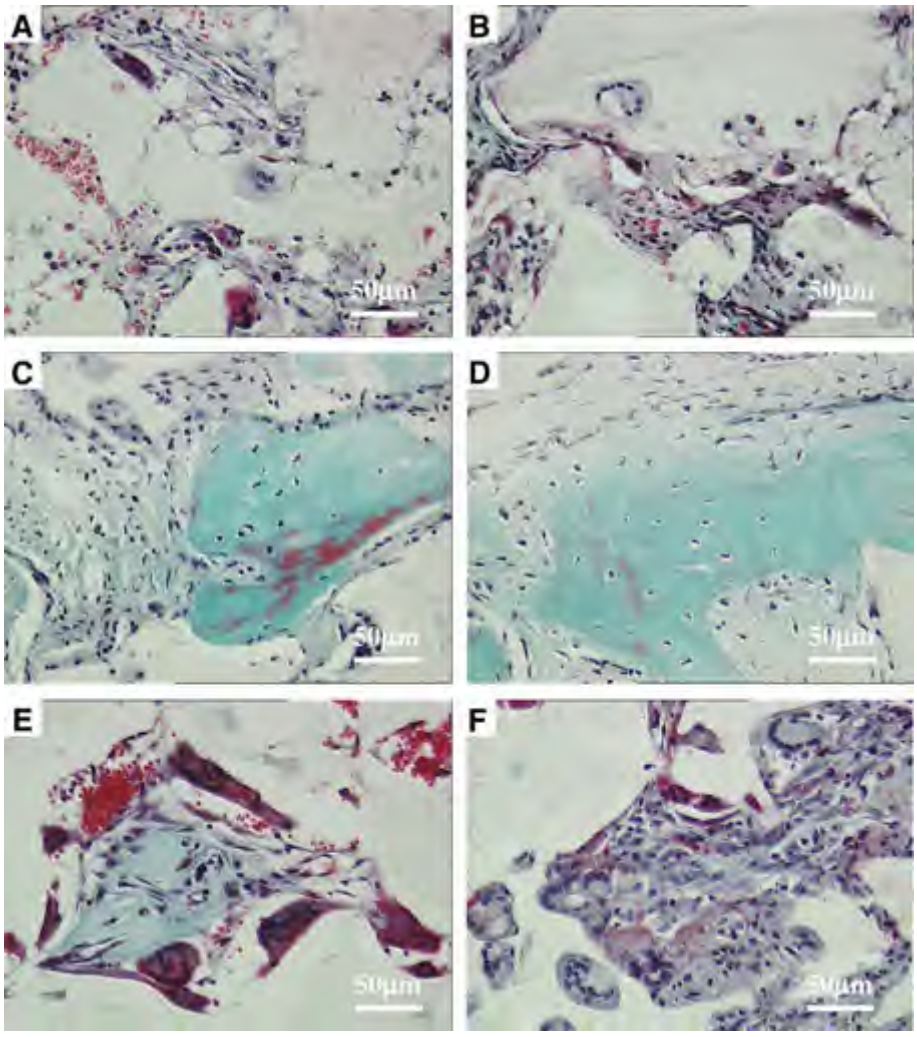

Fig. 9. Masson's trichrome staining photomicrographs (400× magnification) for rabbit radius defects repair of: PLGA (A), 5 wt.% op-HA/PLGA (B), 10 wt.% op-HA/PLGA (C), 20 wt.% op-HA/PLGA (D), 40 wt.% op-HA/PLGA (E) and HA/PLGA (F) 24 weeks postoperatively.

face modification of HA particles with poly(L-lactide) (PLLA) or L-lactic acid oligomer would decrease their mineralization and osteogenesis. However, the composites of grafted HA/PLGA had been expected to possess superior in vivo mineralization and osteogenesis compared to ungrafted HA/PLGA at the same contents of HA particles [19]. Similarly in this study, 10 wt.% op-HA/PLGA exhibited better cell adhesion, proliferation and osteogenesis than 10 wt.% ungrafted HA/PLGA.

This study has also shown that, by altering the op-HA contents to a certain extent, the osteoconductive ability of the op-HA/PLGA composites may be increased in vitro and in vivo. The composites with the contents of 10 and 20 wt.% op-HA exhibited best comprehensive properties. The following possible mechanisms were deduced from the obtained results.

First, the composites with the content of 10–20 wt.% op-HA will provide suitable surface topography for cell attachment and expanding, including proper roughness and a flat surface. It was reported that surface roughness could enhance attachment, proliferation and differentiation of anchorage-dependent bone forming cells [21,24,25]. From the SEM photographs, it was elicited that the surface of pure PLGA was too smooth to allow the osteoblasts to attach well. Meanwhile, the surface of the 40 wt.% op-HA/PLGA was too rough and irregular to prevent the osteoblasts from expanding and immigrating.

Second, the higher mechanical properties and stability of the composite scaffolds could bear better loading ability and provide more stable 3D space for cell growth and extracellular matrix formation [20,33]. The lower mechanical strength in the 5 and 40 wt.% op-HA/PLGA groups will result in earlier corruption of the scaffold architecture, and cell ingrowth and tissue regeneration will be hindered.

Third, pore structures of scaffolds play a critical role in bone formation in vitro and in vivo [33,34]. Higher porosity and pore size result in greater bone ingrowth. The pores of the 10 and 20 wt.% op-HA/PLGA showed well-distributed and higher porosities, which could ensure that new bone ingrows evenly. The pore walls of 40 wt.% op-HA/

PLGA were thicker than the other groups, and this could influence the cell extent and body fluid flow through the pores. Although more micropores distributed in the walls of the composites could provide a larger surface for serum proteins and growth factor deposition, the micropores increasing to an extreme extent in the composite of 40 wt.% op-HA/PLGA could decrease its mechanical properties contrarily.

Lastly, the degradation time of the composite could be prolonged as the contents of op-HA in the composites increased. Although the bioactivity of op-HA will improve the implant treatment by facilitating rapid cell adhesion and migration, and hence enhance bone formation in vivo, the osteogenesis could be hindered as soon as the rate of degradation of the scaffold material no longer matches the rate of remodeling [34].

4. Conclusions

We have reported a novel nanocomposite scaffold of op-HA/PLGA fabricated by the melt-molding and particulate leaching method. Nanohydroxyapatite surface-modified with L-lactic acid oligomer was prepared by LAc oligomer grafted onto the hydroxyapatite surface. The composites of op-HA/PLGA exhibited a series of prospective features, including good biocompatibility, homogeneity and mechanical properties. The mechanical properties, cell attachment and proliferation, and osteogenetic ability of the composites were obviously influenced by the content of op-HA in the composite. The composite scaffolds of 10 and 20 wt.% op-HA/PLGA exhibited better comprehensive properties, and were the optimal bone repairing materials for tissue engineering and orthopedic application.

Acknowledgments

The authors are thankful to the National Natural Science Foundation of China (No. 50673090), National Science Fund for Distinguished Young Scholar (No. 50425309) of China, and the "863" Project (No. 2007AA03Z320) from the Ministry of Science and Technology of China, as well as Major Project of International Cooperation from the Ministry of Science and Technology of China (20071314) for their financial support of this work.

References

[1] Shikinami Y, Okuno M. Bioresorbable devices made of forged composites of hydroxyapatite (HA) particles and poly-L-lactide (PLLA). I. Basic characteristics. Biomaterials 1999;20:859–77.
[2] Petricca SE, Marra KG, Kumta PN. Chemical synthesis of poly(lactic-co-glycolic acid)/hydroxyapatite composites for orthopaedic applications. Acta Biomater 2006;2:277–86.
[3] Kim SS, Park MS, Jeon O, Choi CY, Kim BS. Poly(lactide-co-glycolide)/hydroxyapatite composite scaffolds for bone tissue engineering. Biomaterials 2006;27:1399–409.
[4] Hong ZK, Zhang PB, Liu AX, Chen L, Chen XS, Jing XB. Composites of poly(lactide-co-glycolide) and the surface modified carbonated hydroxyapatite nanoparticles. J Biomed Mater Res A 2007;81:515–22.
[5] Borum L. Wilson Jr. OC. Surface modification of hydroxyapatite. Part II. Silica. Biomaterials 2003;24:3681–8.
[6] Misra DN. Adsorption of zirconyl salts and their acids on hydroxyapatite: use of the salts as coupling agents to dental polymer composite. J Dent Res 1985;12:1405–8.
[7] Liu Q, de Wijn JR, Bakker D, van Toledo M, van Blitterswijk CA. Polyacids as bonding agents in hydroxyapatite polyester-ether (polyactive (TM) 30/70) composites. J Mater Sci Mater Med 1998;9:23–30.
[8] Borum-Nicholas L. Wilson Jr. OC. Surface modification of hydroxyapatite. Part I. Dodecyl alcohol. Biomaterials 2003;24:3671–9.
[9] Wang X, Li Y, Wei J, Groot K. Development of biomimetic nanohydroxyapatite/poly (hexamethylene adipamide) composites. Biomaterials 2002;23:4787–91.
[10] Dong GC, Sun JS, Yao CH, Jiang GJ, Huang CW, Lin FH. A study on grafting and characterization of HMDI-modified calcium hydrogen phosphate. Biomaterials 2001;22:3179–89.
[11] Hong ZK, Qiu XY, Sun JR, Deng MX, Chen XS, Jing XB. Grafting polymerization of L-lactide on the surface of hydroxyapatite nanocrystals. Polymer 2004;45:6699–706.
[12] Qiu XY, Hong ZK, Hu JL, Chen L, Chen XS, Jing XB. Hydroxyapatite surface modified by L-lactic acid and its subsequent grafting polymerization of L-lactide. Biomacromolecules 2005;6:1193–9.
[13] Hong ZK, Zhang PB, He CL, Qiu XY, Liu AX, Chen L, et al. Nano-composite of poly(L-lactide) and surface grafted hydroxyapatite: mechanical properties and biocompatibility. Biomaterials 2005;26:6296–304.
[14] Qiu XY, Chen L, Hu JL, Sun JR, Hong ZK, Liu AX, et al. Surface-modified hydroxyapatite linked by L-lactic acid oligomer in the absence of catalyst. J Polym Sci A Polym Chem 2005;43:5177–85.
[15] Oh SH, Kang SG, Lee JH. Degradation behavior of hydrophilized PLGA scaffolds prepared by melt-molding particulate-leaching method: comparison with control hydrophobic one. J Mater Sci Mater Med 2006;17(2):131–7.
[16] Shi DH, Cai DZ. Development and potential of a biomimetic chitosan/type II collagen scafford for cartilage tissue engineering. Chin Med J 2005;118(17):1436–43.
[17] Gümüşderelioğlu M, Türkoğlu H. Biomodification of non-woven polyester fabrics by insulin and RGD for use in serum-free cultivation of tissue cells. Biomaterials 2002;23:3927–35.
[18] Wilda H, Gough JE. In vitro studies of annulus fibrosus disc cell attachment, differentiation and matrix production on PDLLA/45S5. Bioglass composite films. Biomaterials 2006;27:5220–9.
[19] Zhang PB, Hong ZK, Yu T, Chen X, Jing XB. In vivo mineralization and osteogenesis of nanocomposite scaffold of poly(lactide-co-glycolide) and hydroxyapatite surface-grafted with poly(L-lactide). Biomaterials 2009;30:58–70.
[20] Kothapalli CR, Shaw MT, Wei M. Biodegradable HA-PLA 3-D porous scaffolds: effect of nano-sized filler content on scaffold properties. Acta Biomater 2005;1(6):653–62.
[21] Yuan H, Kurashina K, de Bruijn JD, Li Y, de Groot K, Zhang X. A preliminary study on osteoinduction of two kinds of calcium phosphate ceramics. Biomaterials 1999;20:1799–806.
[22] Verrier S, Blaker JJ, Maquet V, Hench LL, Boccaccini AR. PDLLA/Bioglass composites for soft-tissue and hard-tissue engineering: an in vitro cell biology assessment. Biomaterials 2004;25:3013–21.
[23] Anselme K. Osteoblast adhesion on biomaterials. Biomaterials 2000;21(7):667–81.
[24] Mustafa K, Wroblewski J, Hultenby K, Lopez BS, Arvidson K. Effects of titanium surfaces blasted with TiO_2 particles on the initial attachment of cells derived from human mandibular bone: A scanning electron microscopic and histomorphometric analysis. Clin Oral Implants Res 2000;11:116–28.
[25] Deligianni DD, Katsala N, Ladas S, Sotiropoulou D, Amedee J, Missirlis YF. Effect of surface roughness of the titanium alloy Ti-6A1-

4V on human bone marrow cell response and on protein adsorption. Biomaterials 2001;22:1241–51.
[26] Busa WB, Nuccitelli R. Metabolic regulation via intracellular pH. Am J Physiol Regul Integr Comp Physiol 1984;246: R409–38.
[27] Mokbel N, Bou Serhal C, Matni G, Naaman N. Healing patterns of critical size bony defects in rat following bone graft. Oral Maxillofac Surg 2008;12(2):73–8.
[28] Nie H, Wang CH. Fabrication and characterization of PLGA/HAp composite scaffolds for delivery of BMP-2 plasmid DNA. J Control Release 2007;120:111–21.
[29] Huang J, Best S, Bonfield W, Brooks RA, Rushton N, Jayasinghe SN, et al. In vitro assessment of the biological response to nano-sized hydroxyapatite. J Mater Sci Mater Med 2004;15:441–5.
[30] Pezzatini S, Solito R, Morbidelli L, Lamponi S, Boanini E, Bigi A, et al. The effect of hydroxyapatite nanocrystals on microvascular endothelial cell viability and functions. J Biomed Mater Res A 2006;76:656–63.
[31] Bagambisa FB, Joos U. Preliminary studies on the phenomenological behaviour of osteoblasts cultured on hydroxyapatite ceramics. Biomaterials 1990;11(1):50–6.
[32] Luyten FP, Cunningham NS, Vukicevic S, Paralkar V, Ripamonti U, Reddi AH. Advances in osteogenin and related bone morphogenetic proteins in bone induction and repair. Acta Orthop Belg 1992;58(1):263–7.
[33] Gunatillake PA, Adhikari R. Biodegradable synthetic polymers for tissue engineering. Eur Cells Mater 2003;5:1–16.
[34] Karageorgiou V, Kaplan D. Porosity of 3D biomaterial scaffolds and osteogenesis. Biomaterials 2005;26:5474–91.